



Spectroscopic and Magnetic Study of Mixed Ligand Complexes with Divalent Transition Metals Using Azo-Azomethine Ligands

Ali Hussein Mohammed Alwan

General Directorate of Education of Thi Qar governorate - Specialist Supervision
Department

al.hu_ch@utq.edu.iq

<https://doi.org/10.32792/utq/utj/vol20/2/1>

Abstract

The research involves the synthesis and characterization of a number of mixed ligand complexes with divalent cobalt, nickel, copper, and zinc ions, using a new homocyclic azo-azomethine ligand 1-(4-(1-(p-tolylamino) ethyl) phenyl) diazanyl) naphthalen-2-ol (TEPDN) and two organic ligands: HL2 (o-aminophenol) and HL3 (anthranilic acid). The results indicated that the mixed ligand complexes have a molar ratio of (metal:ligand) (1:1:1). The spatial structures of the mixed ligand complexes were proposed based on the results of UV-Vis spectroscopy, in addition to magnetic susceptibility and molar conductivity measurements of the synthesized chelated complexes. Tetrahedral geometries were suggested for the cobalt (II) and zinc (II) complexes, while square planar geometries were proposed for the nickel (II) and copper (II) complexes.

Keywords: mixed ligand, characterization, azomethine

Introduction

Azo-azomethine compounds and their complexes are of significant importance, as they have garnered the attention of researchers and scientists due to their numerous pharmaceutical applications, particularly as antibacterial and antifungal agents ⁽¹⁾. Some of these compounds, when reacted with cellulose, produce colored cellulose fibers with high stability when exposed to light and heat ⁽²⁾. The effectiveness of this type of ligand is attributed to the nitrogen atom present in both the azo and azomethine functional groups, in addition to other groups such as hydroxyl, carboxyl, and amine. The coordination methods of these ligands with metal ions vary depending on the nature of the ligand, in terms of the number of donor atoms qualified for coordination and their positions relative to the azo and azomethine groups ⁽³⁾. This research includes the synthesis and characterization of an azo-azomethine ligand (TEPDN) and a number of mixed ligand complexes derived from this ligand with several divalent metal ions.



Experimental Section

Materials and Instruments

High-purity materials supplied by B.D.H, Fluka, and GCC companies were used. The melting and decomposition points of the prepared solid compounds were measured using the Stuart Melting Points SMP10 device. Molar electrical conductivity was measured using a Digital Conductivity Series Ino.Lab.720 device at a concentration of (1×10^{-3} M) using ethanol as a solvent. Additionally, magnetic susceptibility of the prepared complexes was measured using a Balance Magnetic Susceptibility Model-M.S.B Auto via the Faraday method, with diamagnetic corrections applied using Pascal constants⁽⁴⁾. The electronic spectra of the prepared complexes were recorded at room temperature in ethanol solvent using a Shimadzu UV-1700 spectrophotometer. Infrared spectra were obtained using KBr discs on a Shimadzu FTIR 8400S spectrophotometer in the range of ($400-4000 \text{ cm}^{-1}$) in terms of wavenumber. Elemental analysis was performed to determine the carbon, hydrogen, and nitrogen content in the prepared ligand and mixed ligand complexes using a C.H.N. EA-034 mt analyzer. Some physical properties of the ligands and the prepared mixed ligand complexes are listed in Table 1.

Synthesis of the TEPDN Ligand

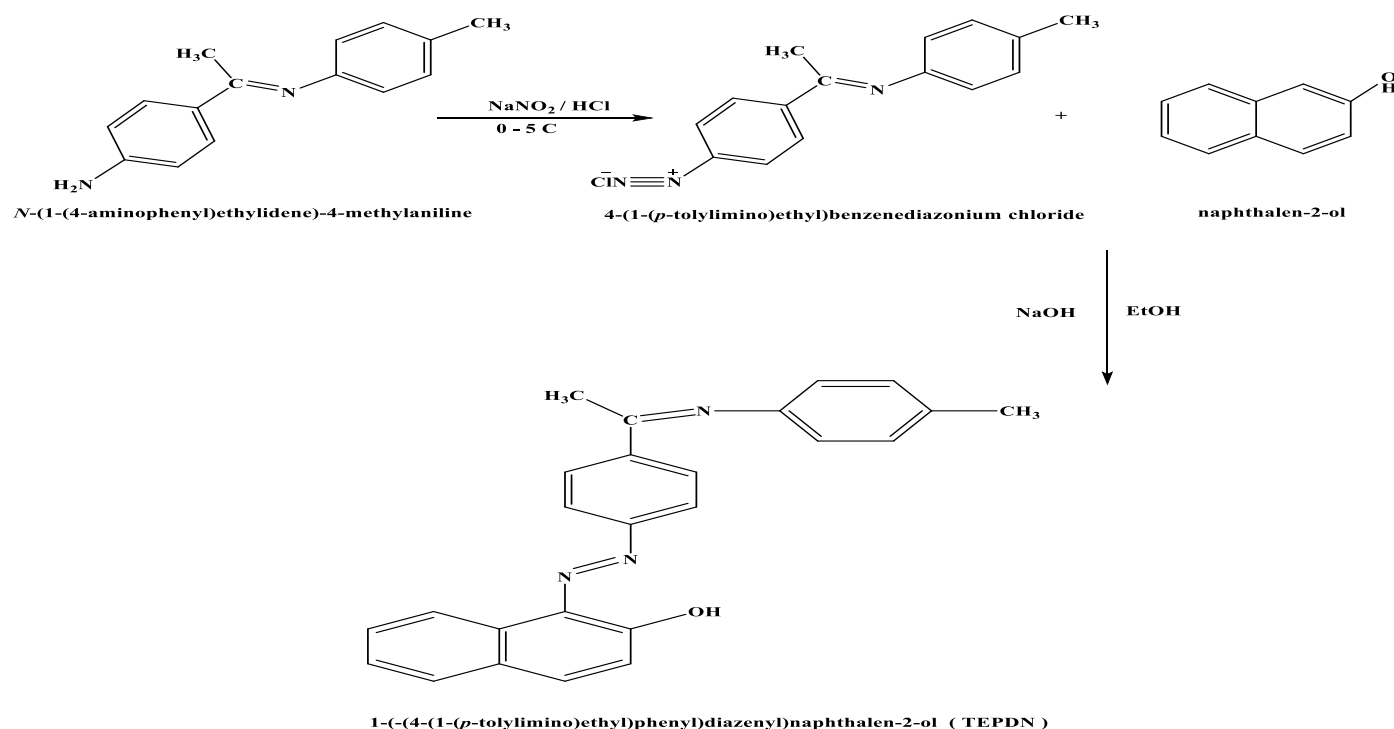
The homocyclic azo-azomethine ligand 1-(4-(1-(p-tolylamino) ethyl) phenyl) diazanyl) naphthalen-2-ol (TEPDN) was synthesized in two steps. The first step involved a condensation reaction between p-aminoacetophenone and an equimolar amount (1:1) of p-toluidine, both dissolved in ethanol. Three drops of glacial acetic acid were added, followed by heating the mixture for 6 hours to obtain the Schiff base. In the second step, diazotization and coupling reactions were carried out by dissolving 10 mmol (2.24 g) of N-(1-(4-aminophenyl) ethylidene)-4-methylaniline in 20 mL of ethanol. Then, 3 mL of 11M hydrochloric acid and 20 mL of distilled water were added. The mixture was cooled to a temperature between 0-5°C. A solution of 0.75 g (10 mmol) sodium nitrite dissolved in 10 mL of distilled water was added dropwise with continuous stirring, ensuring the temperature did not exceed 5°C. The solution was left to stand for 15 minutes to complete the diazotization process.

The diazonium solution was added dropwise with continuous stirring to a solution of 1.44 g (10 mmol) of β -naphthol dissolved in a mixture of 100 mL of ethanol and 50 mL of 10% sodium hydroxide solution. The solution turned orange upon addition. The reaction mixture was left overnight, and the pH was adjusted by adding hydrochloric acid until reaching neutrality. An orange precipitate formed, which was allowed to settle. The precipitate was filtered and washed with distilled water to remove the sodium chloride formed during the neutralization process. After ensuring the absence of residual salt, the

precipitate was air-dried and recrystallized from hot ethanol. The collected precipitate was then dried in an oven at 80°C for 24 hours. Scheme 1 illustrates the reaction pathway.

Synthesis of Metal(II) Complexes

The complex [ML₁L₂] was synthesized by adding 0.5 mmol of metal chloride salts dissolved in 25 mL of ethanol to a mixed ligand solution containing 0.5 mmol of both ligands (HL₁, HL₂). Similarly, the complex [ML₁L₃] was prepared using 0.5 mmol of ligands (HL₁, HL₃) following the same procedure.



Scheme 1 illustrates the reaction pathway.

Results and Discussion

Table 1 presents some physical properties of the ligand (TEPDN) and the synthesized mixed ligand complexes. The metal content in the complexes was determined using atomic absorption spectroscopy. All the synthesized complexes are insoluble in water but are readily soluble in hot ethanol and completely



dissolve in dimethyl sulfoxide (DMSO). The molar electrical conductivity values of the prepared complexes ranged between 8.37 and 14.12 $\text{S}\cdot\text{cm}^2\cdot\text{mol}^{-1}$, indicating non-ionic nature of the complexes, and thus, these complexes are non-conductive.⁽⁵⁾

Mass Spectrometry Analysis

The mass spectra of the ligand (TEPDN) and the mixed ligand complexes were recorded at room temperature. The mass spectrum of the ligand shows a peak at 379 m/z, representing the molecular ion of the ligand. The molecular ion peak for the copper(II) complex (M8) is observed at 579 m/z, which corresponds to the calculated molecular weight of this complex. The mass spectra for the ligand (TEPDN) and the copper complex (M8) are illustrated in Figures 1 and 2.

Infrared Spectroscopy

The absorption bands in the infrared region for the functional groups of the ligands and the mixed ligand complexes are listed in Table 2. A band at 1676 cm^{-1} is attributed to the stretching frequency of the azomethine group in the ligand (TEPDN). No significant changes were observed in the stretching frequency of the (C=N) group in all the complexes⁽⁶⁾. A broad band within the range of $3200\text{-}3520\text{ cm}^{-1}$ is observed, resulting from the stretching frequencies⁽⁷⁾ of the (O-H) and (N-H) bonds. According to sources, the overlap of these absorption bands results in a broad absorption in the range of $3000\text{-}3600\text{ cm}^{-1}$, also attributed to the stretching vibrations of lattice water molecules⁽⁸⁾. The broad band in the region of 1598 cm^{-1} represents the stretching frequency of the (N=N) bond of the prepared ligand, and upon coordination with the metal, it shifts to lower frequencies ($1540\text{-}1580\text{ cm}^{-1}$), indicating the coordination of the azo group with the metal ion⁽⁹⁾. The (M-N) absorption bands were observed in all the complexes in the range of $487\text{-}500\text{ cm}^{-1}$, while the (M-O) absorption bands appeared in the range of $580\text{-}590\text{ cm}^{-1}$, confirming the coordination of metal ions with the ligands through the oxygen atom⁽¹⁰⁾.

Magnetic Measurements and Electronic Spectra

In our study, the ultraviolet-visible (UV-Vis) spectrum of the prepared ligand, dissolved in absolute ethanol, showed absorption peaks in the non-visible range of the spectrum at wavelengths (227-286) and (317-488) nm. These peaks were attributed to the electronic transitions ($\pi\rightarrow\pi^*$) and ($^*\pi\rightarrow n$) of the



aromatic systems connected through the azo bridge⁽¹¹⁾, as well as to the electronic transitions of non-bonding electron pairs on certain atoms carrying these pairs⁽¹²⁾.

Absorption Spectra of the Complexes

The cobalt(II) complexes exhibited two strong absorption peaks (480-488) nm in the visible region, attributed to the (M→L) charge transfer transitions. The coordination of the cobalt ion in the prepared complexes is tetrahedral high-spin, which is consistent with the magnetic susceptibilities measured for the cobalt complexes, BM (3.63, 4.42). In the case of the nickel complexes, an absorption peak was observed in the visible region at 488 nm, attributed to the d-d electronic transitions within the metal itself, specifically the 1A1g→1B1g transition. The nickel complexes showed diamagnetic properties, which aligns with literature reports on square planar nickel complexes⁽¹³⁾. For the copper mixed ligand complexes, two absorption peaks were observed at wavelengths (490, 508) nm, attributed to charge transfer (C.T). The copper complexes showed magnetic moment values ranging between BM (1.37-1.42), confirming a tetrahedral coordination with a square planar⁽¹⁴⁾ arrangement. The absorption peak at 488 nm for the zinc complexes is attributed to the (M→L) charge transfer transition, with diamagnetic properties.

Thermal Analysis

The thermal behavior of the ligand (TEPDN) and some of the mixed ligand complexes was studied using Thermogravimetric Analysis (TGA) over a temperature range of 50-900°C. No significant change in the mass of the ligand was observed below 280°C, indicating the high stability of the ligand. The TGA results are presented in Table 3. For the copper complex (M5), the loss of water of crystallization occurred in the temperature range of 50-145°C, which aligns with literature reports⁽¹⁵⁾ that indicated water loss occurs between 50-280°C. Above 280°C, the loss of coordination water was observed. The high stability of the copper complex (M1) below 290°C suggests the absence of any water molecules in the complex.



No.	Chemical formul	Symbole	M. wt	m.p ⁰ C	Color	Yiel	Found (calc.) %
-----	-----------------	---------	-------	--------------------	-------	------	-----------------

Table 1: Some Physical Properties of the Ligands (HL1 = TEPDN) and (HL2, HL3) and Their Synthesized

Chelated Complexes

							C	H	N	M
1	(C ₂₅ H ₂₁ N ₃ O) =HL ₁	(TEPDN)	379	176-177	Orange	78	76.83 (79.13)	5.42 (5.58)	10.89 (11.07)	-----
2	(C ₆ H ₇ NO) = HL ₂	2-Amino-phenol	109.13	105.28	Pale brown	----	----	----	----	----
3	(C ₇ H ₇ NO ₂) = HL ₃	2-Amino-benzoic acid	137.14	177.95	White	----	----	---	---	----
4	[Cu (C ₃₁ H ₂₆ N ₄ O ₂)]	M ₁	549.13	297-299	Black	76	67.53 (67.68)	4.61 (4.76)	9.93 (10.18)	11.25 (11.55)
5	Co (C ₃₁ H ₂₆ N ₄ O ₂)].2H ₂ O [M ₂	581.23	>300	Black	80	63.87 (64.03)	5.09 (5.20)	9.41 (9.63)	9.81 (10.13)
6	[Ni (C ₃₁ H ₂₆ N ₄ O ₂)].H ₂ O	M ₃	562.72	207-205	Brown	82	65.88 (66.10)	4.89 (5.01)	9.76 (9.95)	10.15 (10.42)
7	Zn (C ₃₁ H ₂₆ N ₄ O ₂)].2H ₂ O [M ₄	587.97	190-191	Dark brown	78	63.11 (63.32)	5.02 (5.14)	9.27 (9.53)	10.98 (11.12)
8	Cu (C ₃₂ H ₂₆ N ₄ O ₃)].4H ₂ O [M ₅	650.12	198-199	Black	79	58.91 (59.11)	5.13 (5.27)	8.46 (8.62)	9.58 (9.77)
9	Co (C ₃₂ H ₂₆ N ₄ O ₃)].2H ₂ O [M ₆	609.51	165-166	Dark orange	82	62.87 (63.05)	4.84 (4.96)	8.82 (9.19)	9.72 (9.67)
10	[Ni (C ₃₂ H ₂₆ N ₄ O ₃)].H ₂ O	M ₇	591.27	183-185	Light orange	78	64.78 (65.00)	4.65 (4.77)	9.21 (9.48)	9.61 (9.93)
11	Zn (C ₃₂ H ₂₆ N ₄ O ₃)].2H ₂ O [M ₈	615.98	170-172	Light brown	80	62.17 (62.39)	4.78 (4.91)	8.93 (9.10)	10.39 (10.62)

Table 2: Infrared Spectra Frequencies of the Ligands and Their Complexes

Compounds	$\nu(\text{O-H})$ H ₂ O hyd-	$\nu(\text{C-H})_{\text{or}}$	$\nu(\text{C-H})_{\text{al}}$	$\nu(\text{N-H})$	$\nu(\text{C=N})$	ν (N=N)	$\nu(\text{C-O})$	$\nu(\text{M-N})$	$\nu(\text{M-O})$
HL ₁	3442 w	3047 w	2958 w	-----	1676 m	1598 w	1203	---	---
HL ₂	3373w	3057 w	-----	3306	-----	-----	1217	-----	-----
HL ₃	3323 w	3050 w	-----	3238	-----	-----	1668	-----	-----
[CoL ₁ L ₂].2H ₂ O	3408 w	3055 w	2960 w	3186	1676 m	1587 w	1203	501 w	580 w
[NiL ₁ L ₂].H ₂ O	3381 w	3059 w	2954 w	3327	1674 m	1563 w	1203	493 w	588 w

[CuL ₁ L ₂]	-----	3057 w	2960 w	3423	1676 m	1583w	1201	486 w	582 w
[ZnL ₁ L ₂].2H ₂ O	3522 w	3055 w	2920 w	3388	1670 m	1566w	1205	487 w	590 w
[CoL ₁ L ₃].2H ₂ O	3481 w	3057 w	3000 w	3421	1674 m	1539 w	1597	5489w	584 w
[NiL ₁ L ₃].H ₂ O	3483 w	3059 w	2875 w	3408	1680 m	1544 w	1597	499 w	588 w
[CuL ₁ L ₃].4H ₂ O	3423 w	3055 w	2935 w	3176	1678 m	1530 w	1600	501 w	582 w
[ZnL ₁ L ₃].2H ₂ O	3522 w	3055 w	2920 w	3388	1670 m	1566 w	1598	487 w	590 w

Table 3: Thermogravimetric Analysis (TGA) Results for the Ligand (HL1) and the Mixed Ligand Complexes (M1) and (M5)

Compound (M.Wt)	Dissociation stages	Temp.range In TG (C°)	Weight loss Found (calc.)	Decomposition Assignment
(C ₂₅ H ₂₁ N ₃ O) =HL ₁ (379)	Stage I Stage II	50 – 280 290 – 577	4.21 (4.23) 61.48(62.26)	Loss of (CH ₄) Loss of(C ₁₅ H ₁₄ N ₃)
[Cu(C ₃₁ H ₂₆ N ₄ O ₂)] = M ₁ (549)	Stage I	50 – 299.5	7.63 (8.17)	Loss of (C ₂ H ₇ N)
[Cu(C ₃₁ H ₂₆ N ₄ O ₂)].4H ₂ O = M ₅ (650)	Stage I Stage II	50 – 145 155 – 299	10.7 (11.07) 25.48 (26.1)	Loss of (4H ₂ O) Loss of (C ₁₀ H ₆ N ₂ O)

Table 4: UV-Visible Spectroscopy and Magnetic Susceptibility Results for the Mixed Ligand Complexes Under Study

Compound	Assigument	Absorption band(n.m)	μ _{eff} (B.M)	Proposed Structure
----------	------------	----------------------	------------------------	--------------------

HL ₁	n→π* & π→π*	317 , 488 227 , 286	----	----
HL ₂	n→π* π→π*	302 274	----	----
HL ₃	n→π* π→π*	336 260	----	----
[Cu (L ₁)(L ₂)]	C. T.	490	1.42	Sq.P
[Co(L ₁)(L ₂).2H ₂ O]	C. T.	488	4.42	Td
[Ni(L ₁)(L ₂).H ₂ O]	¹ A _{1g} → ¹ B _{1g}	489	Dia	Sq.P
[Zn(L ₁)(L ₂).2H ₂ O]	C. T.	488	Dia	Td
[Cu(L ₁)(L ₃).4H ₂ O]	C. T.	508	1.37	Sq.P
[Co(L ₁)(L ₃).2H ₂ O]	C. T.	488	3.63	Td
[Ni(L ₁)(L ₃).H ₂ O]	¹ A _{1g} → ¹ B _{1g}	487	Dia	Sq.P
[Zn(L ₁)(L ₃).2H ₂ O]	C. T.	489	Dia	Td

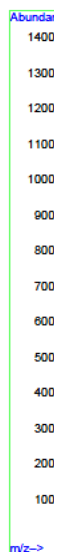


Figure 1: Mass Spectrum of the Ligand (TEPDN)

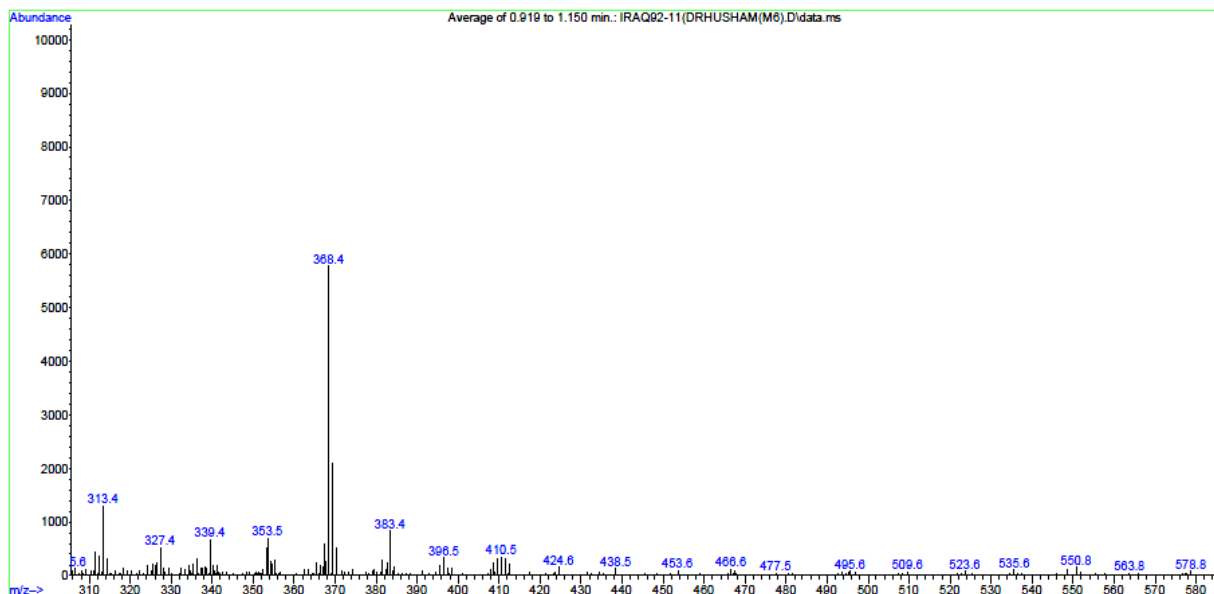


Figure 2: Mass Spectrum of the Mixed Ligand Complex (M8)

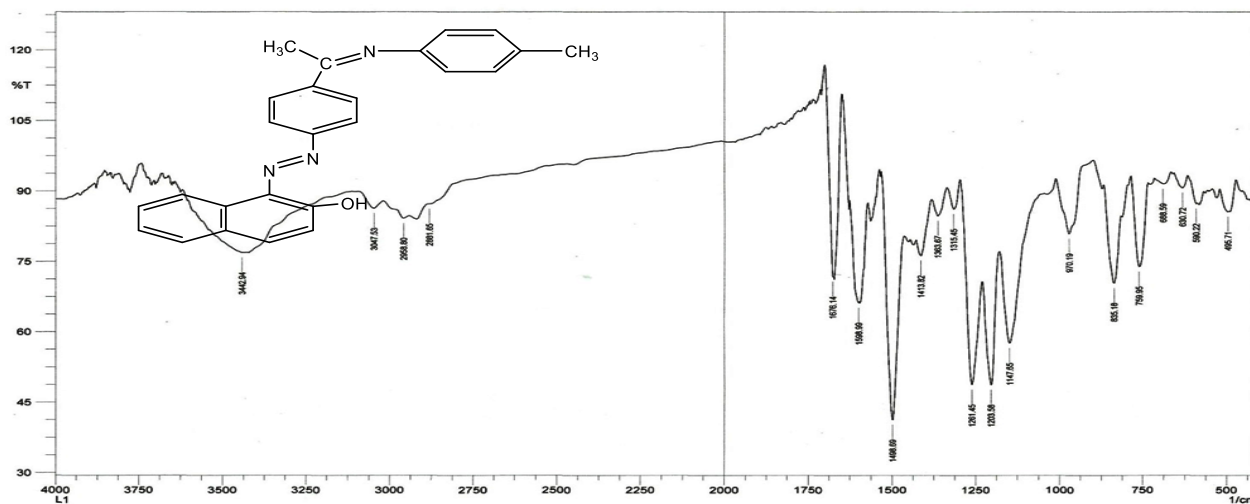


Figure 3: FT-IR Spectrum of the (HL₁) Ligand

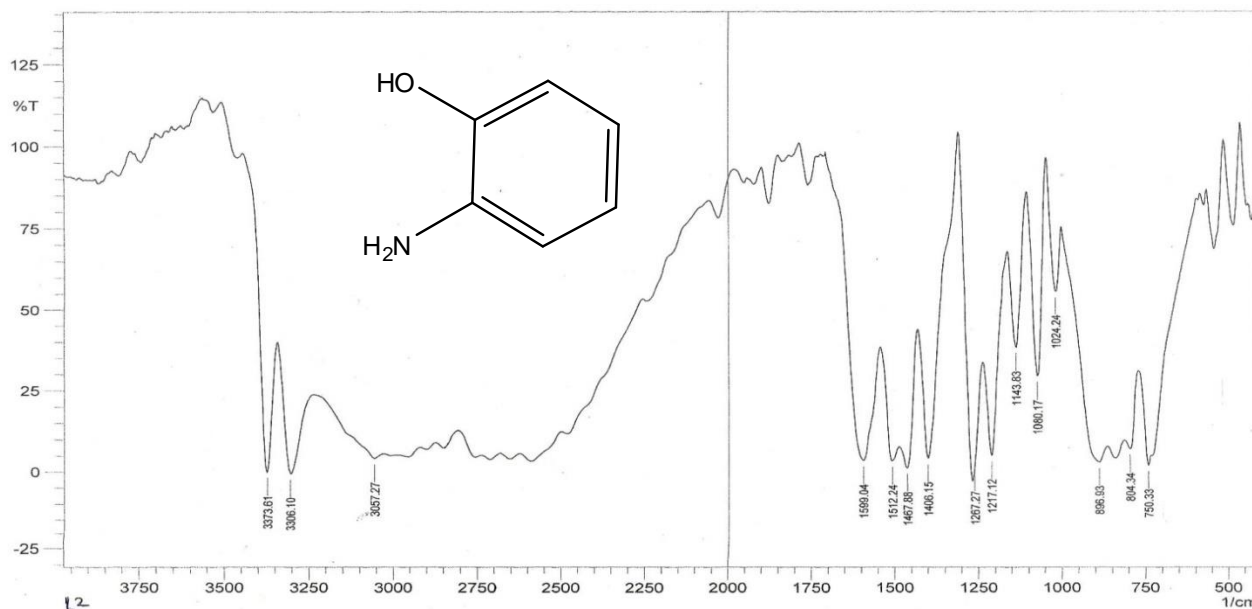


Figure 4: FT-IR Spectrum of the (HL₂) Ligand

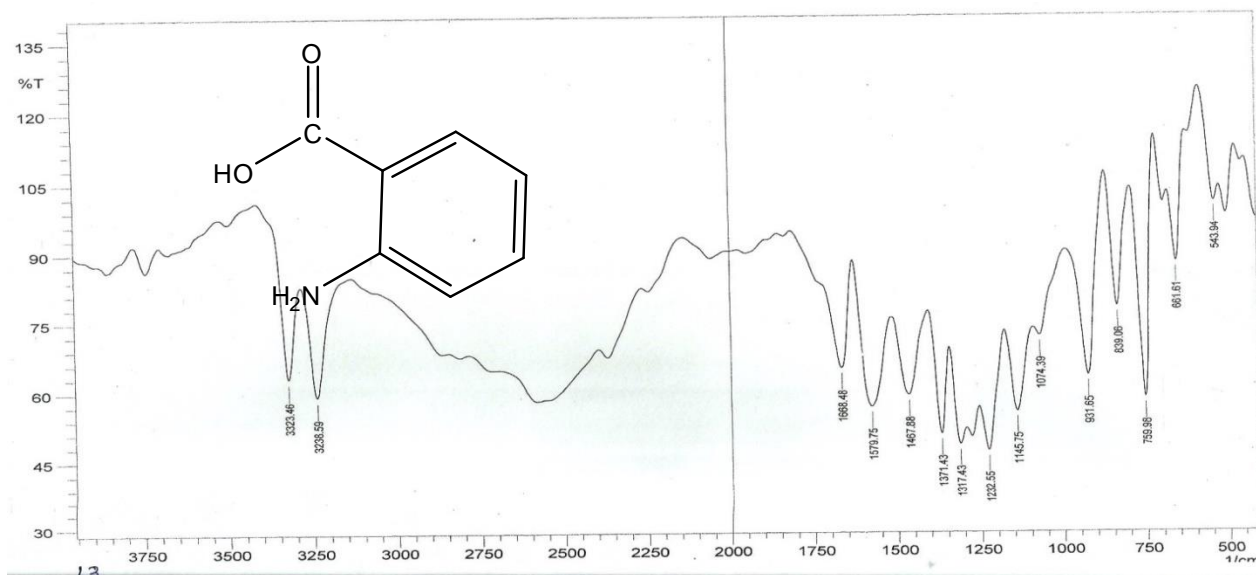


Figure 5: FT-IR Spectrum of the (HL₃) Ligand

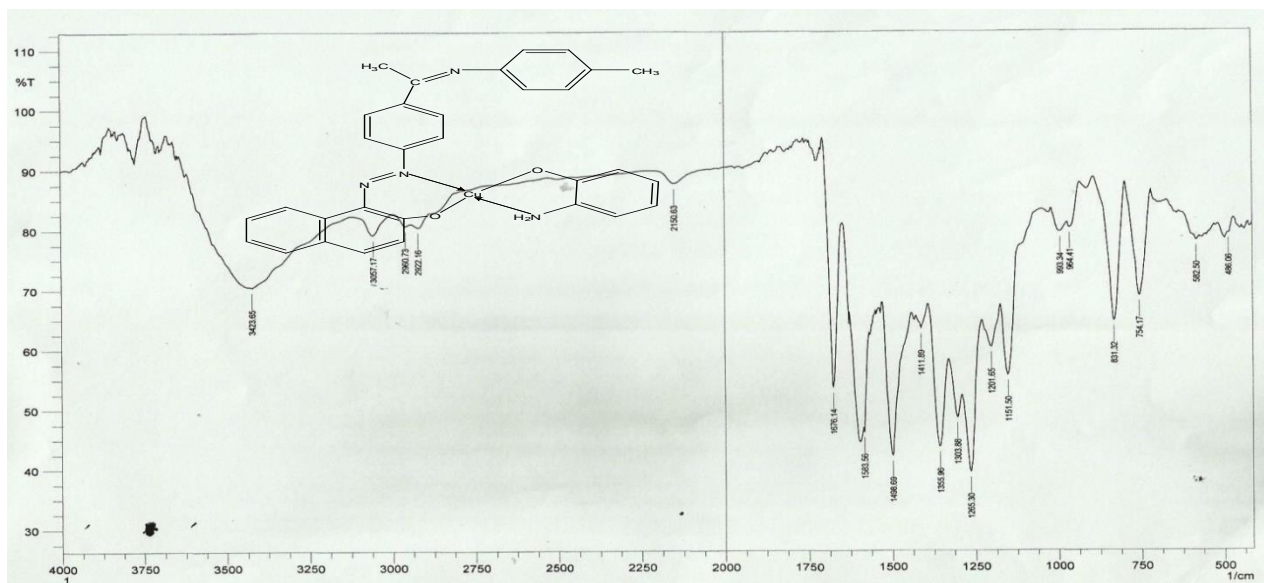


Figure 6: FT-IR Spectrum of the mixed Ligand complex [Cu (L1)(L2)].

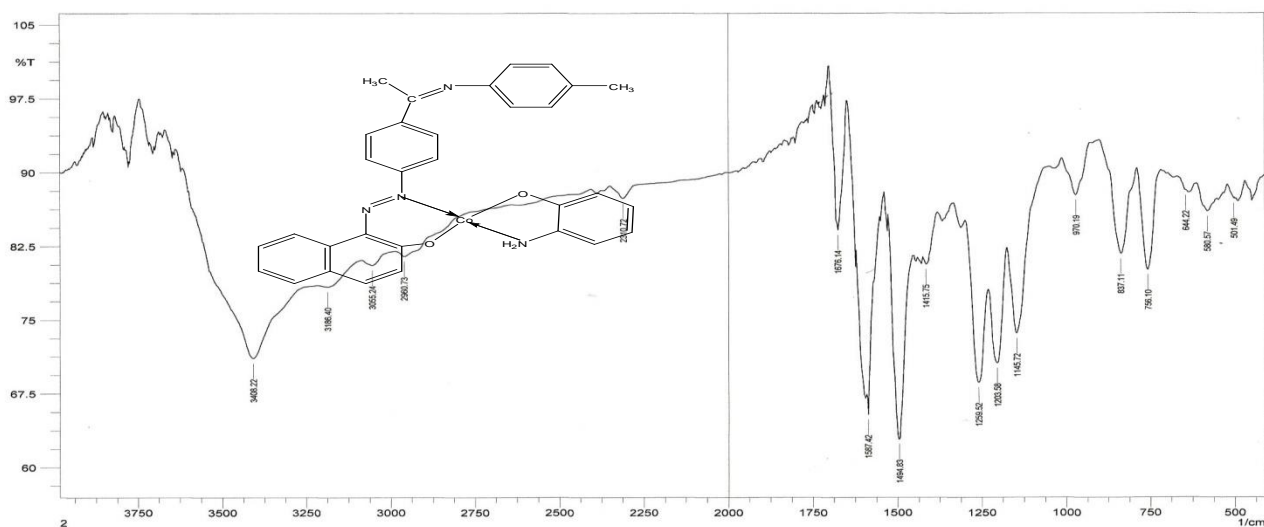


Figure 7: FT-IR Spectrum of the mixed Ligand complex . [Co (L1)(L2)] 2H2O.

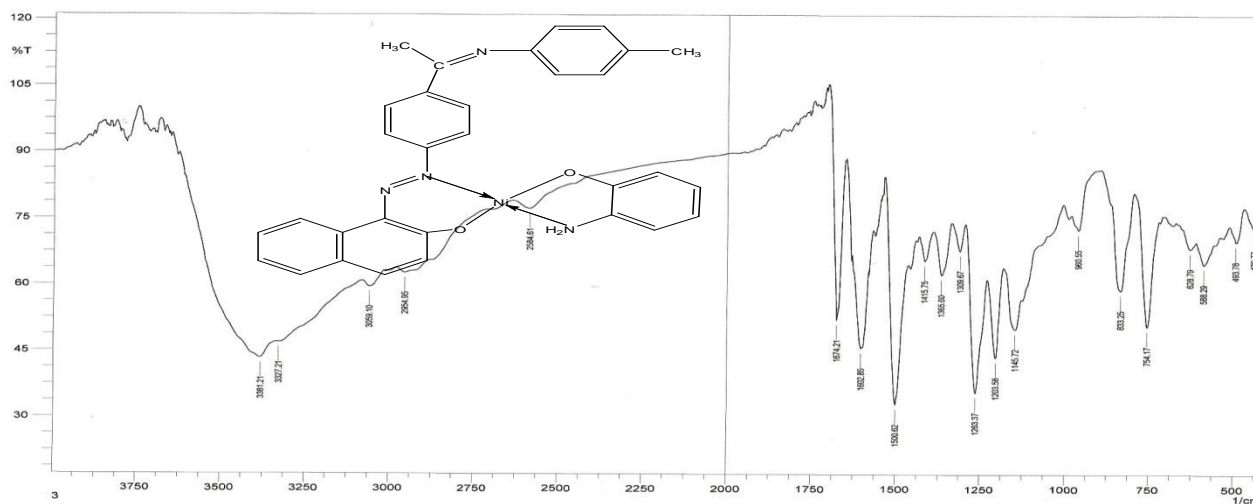


Figure 8: FT-IR Spectrum of the mixed Ligand complex . $[Ni(L1)(L2)] H_2O$.

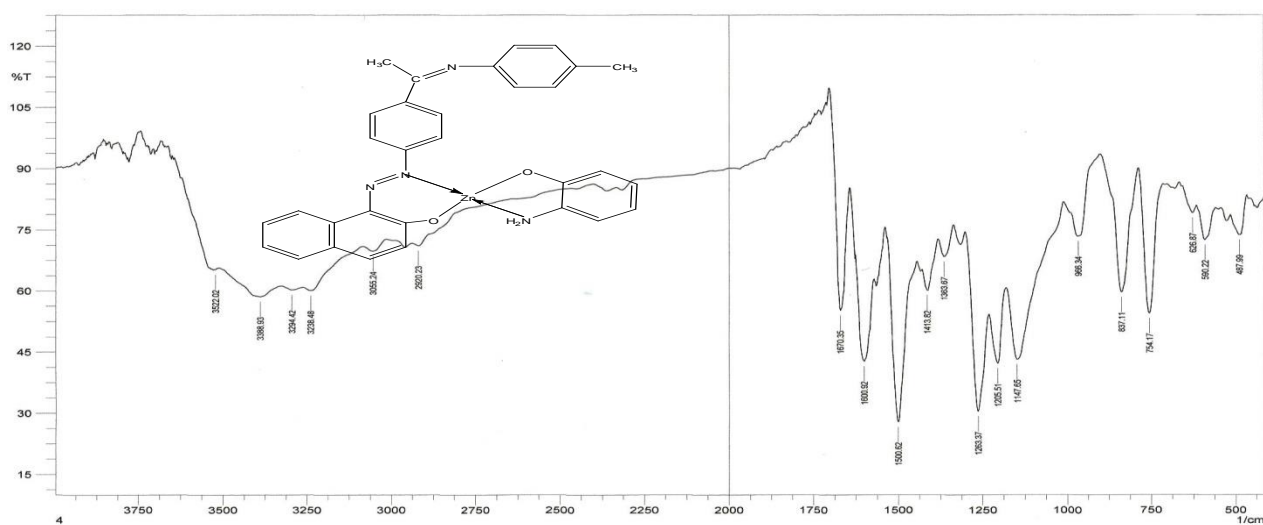


Figure 9: FT-IR Spectrum of the mixed Ligand complex . $[Zn(L1)(L2)]_2 H_2O$.

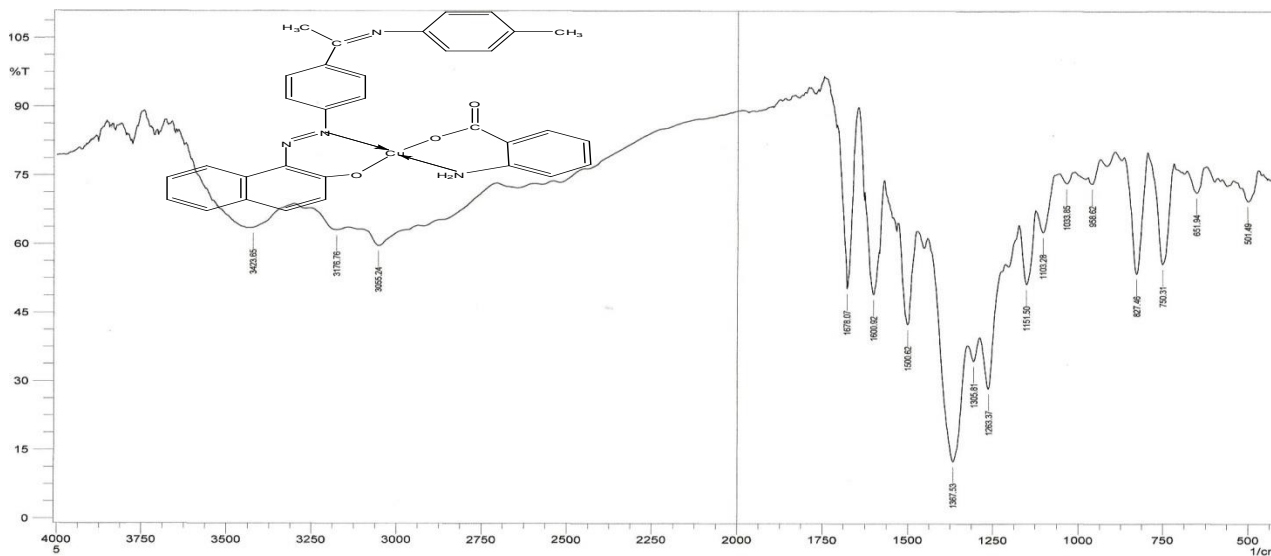


Figure 10: FT-IR Spectrum of the mixed Ligand complex . $[Cu(L1)(L2)]4H_2O$.

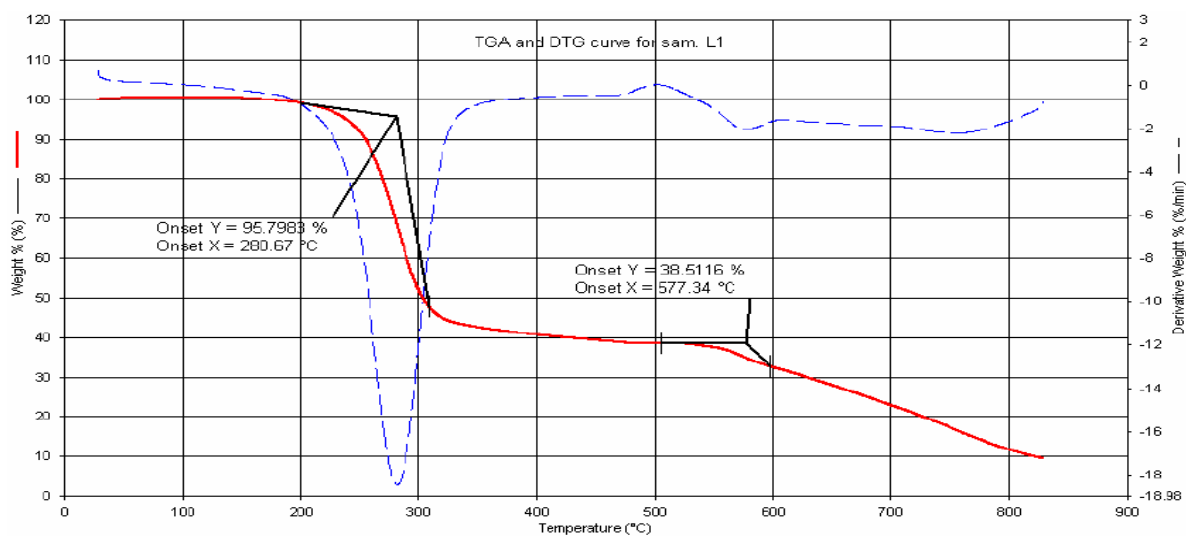


Figure 11 : TGA of the(HL_1) Ligand

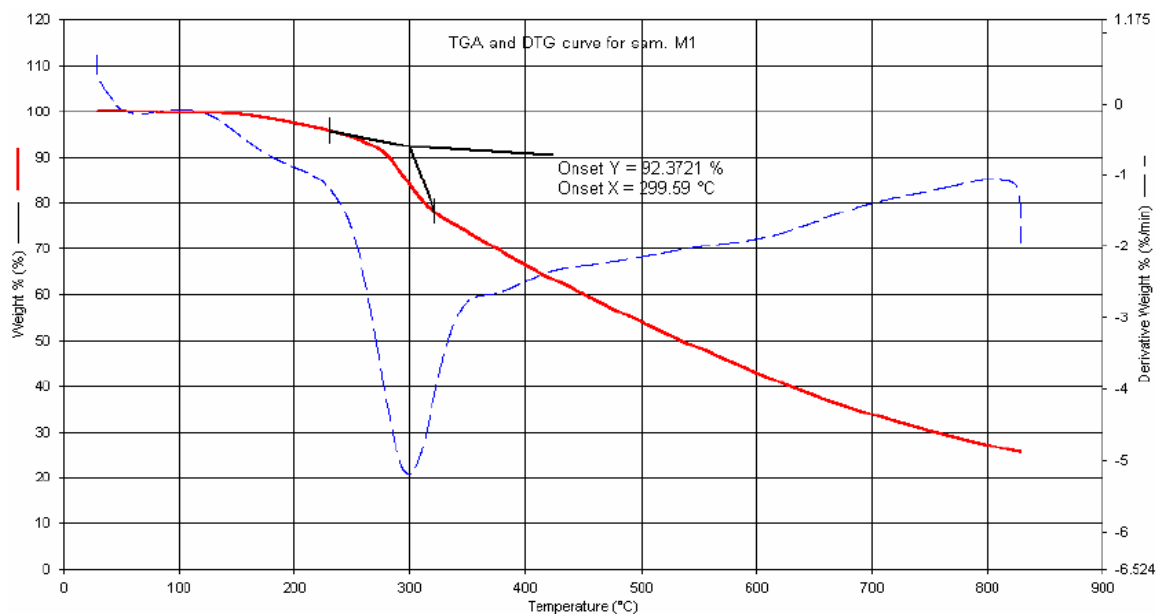


Figure 12 : TGA of the mixed Ligand complex [Cu(L1)(L2)]

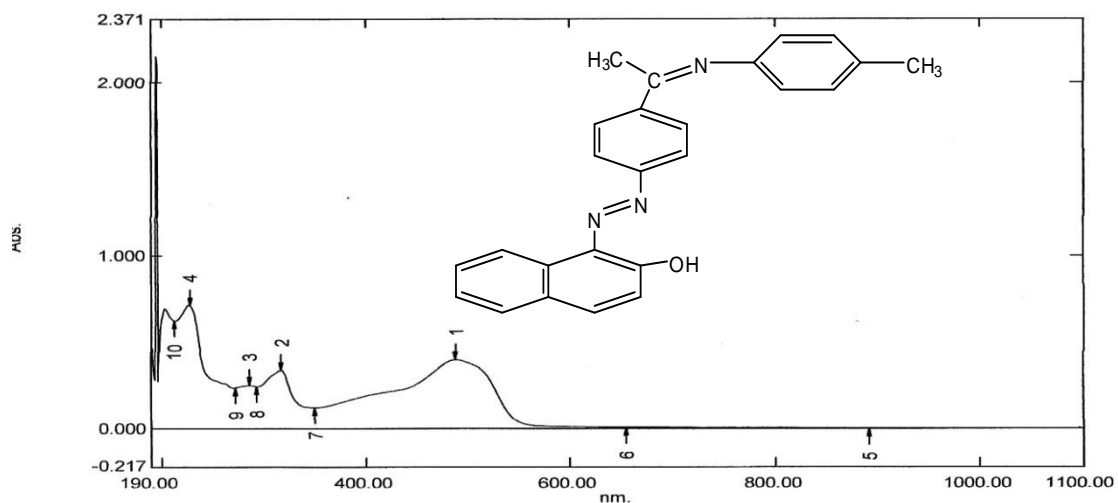


Figure 13 : Electronic spectrum of (HL₁)

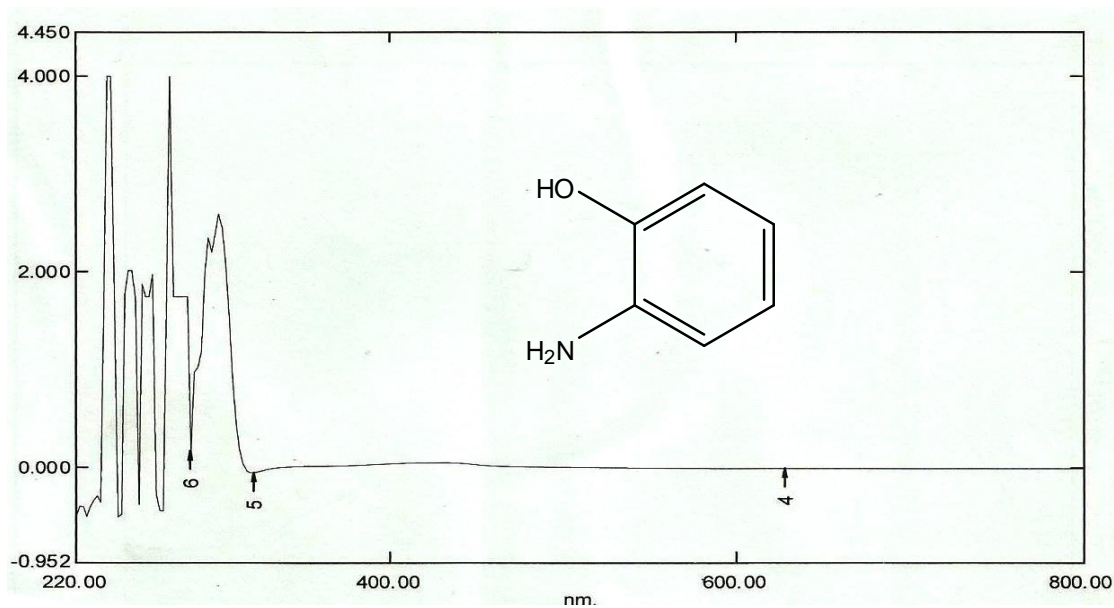


Figure 14 : Electronic spectrum of (HL₂)

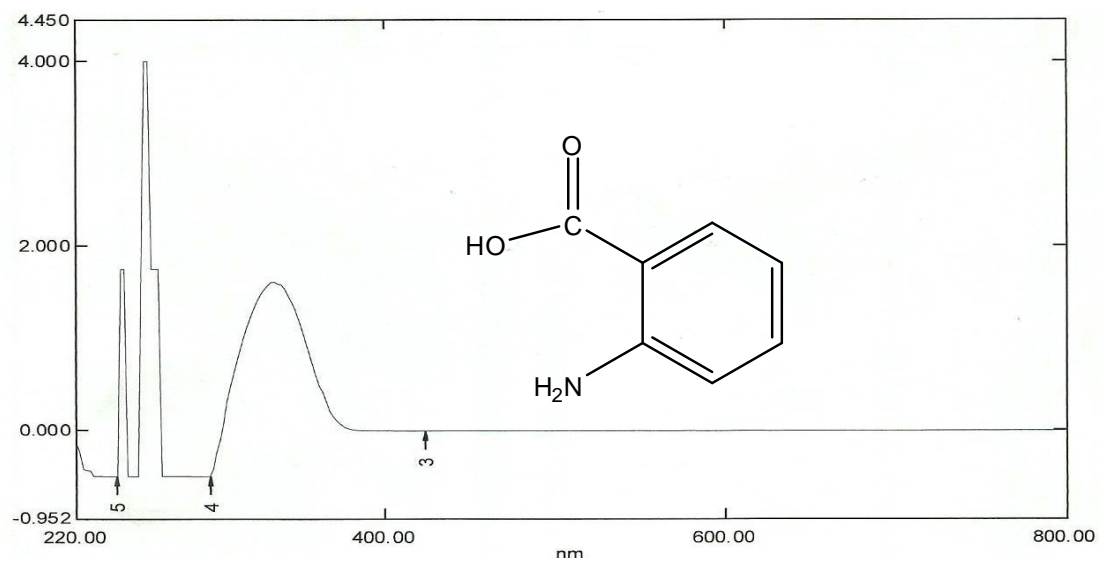


Figure 15 : Electronic spectrum of (HL₃)

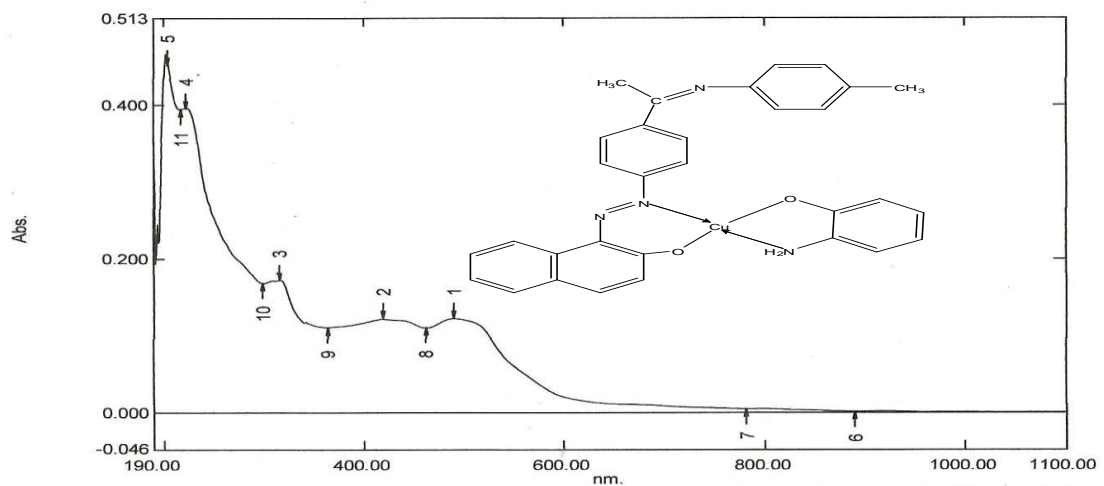


Figure 16 : Electronic spectrum of mixed ligand complex ($\text{Cu}(\text{L}_1)(\text{L}_2)$)

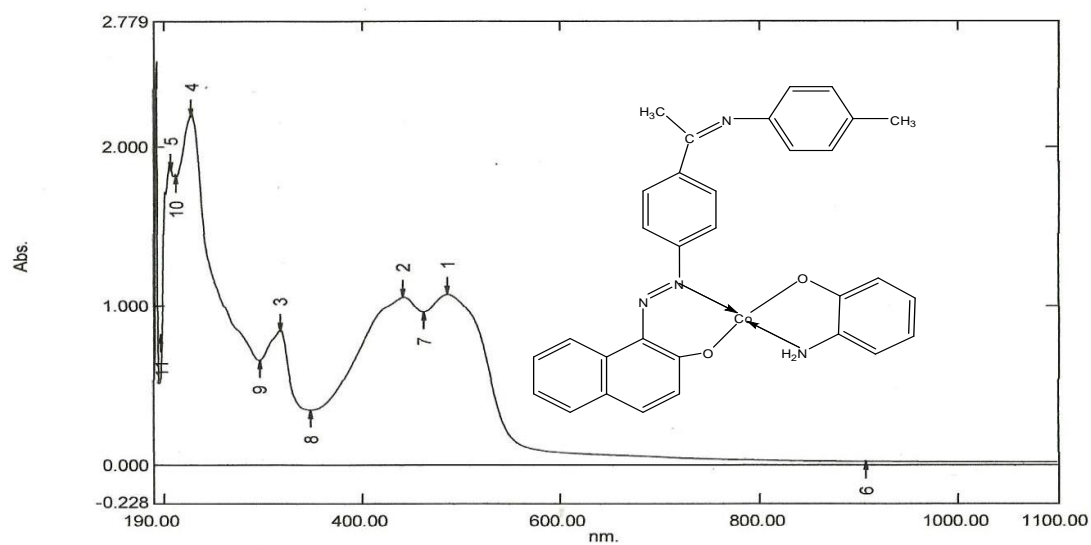


Figure 17 : Electronic spectrum of mixed ligand complex $[\text{Co}(\text{L}_1)(\text{L}_2)] \cdot 2\text{H}_2\text{O}$

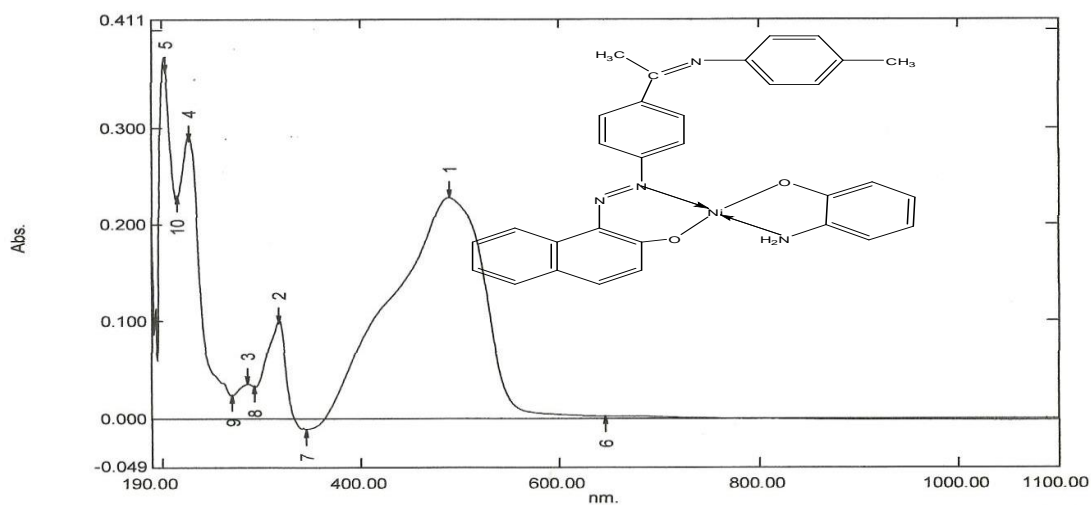


Figure 18 : Electronic spectrum of mixed ligand complex [Ni(L1)(L2)].H₂O

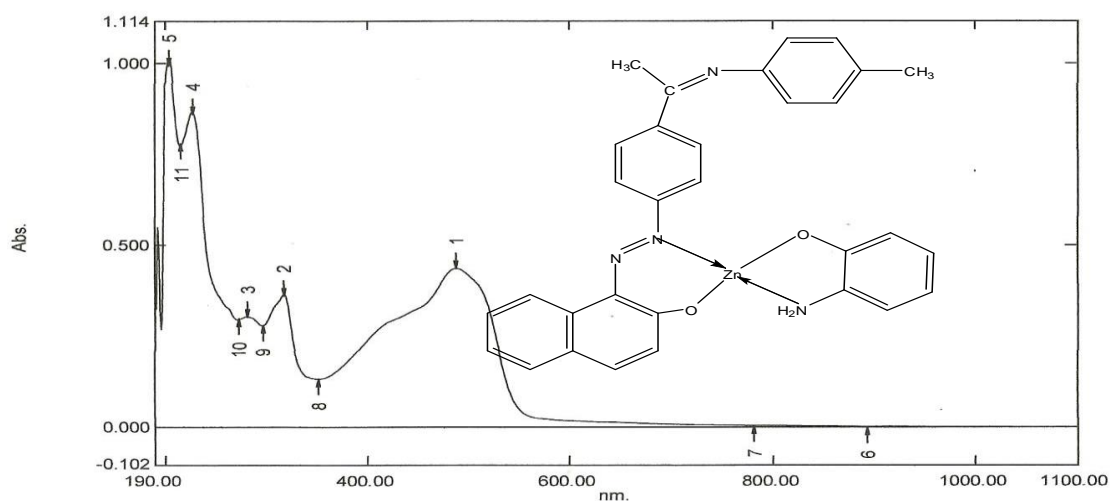


Figure 19 : Electronic spectrum of mixed ligand complex [Zn(L1)(L2)].H₂O



References:

1. H. A. M. Al-Zahrani, M. S. Al-Juaid, and M. S. Alam; *Int. J. Chem. Technol. Res.*, 14(4), 182-192 (2021).
2. Y. Wang, H. Liu, Y. Xu, and Z. Yang; *J. Chem. Eng. Data*, 67(6), 1820-1829 (2022).
3. M. P. Rosu, D. C. M. Pritschow, and V. H. Zang; *Coord. Chem. Rev.*, 454, 214-229 (2022).
4. S. N. Basha, R. S. Jadhav, and S. V. Suryawanshi; *Int. J. Pharm. Tech. Res.*, 13(2), 105-115 (2020).
5. L. M. Silva, T. E. Sant'Anna, and C. M. Rodrigues; *New J. Chem.*, 45(3), 1198-1206 (2021).
6. R. K. Sharma, P. K. Singh, and M. K. Rao; *J. Chem. Research*, 46(6), 400-409 (2022).
7. A. S. Kumar, R. P. Tiwari, and N. R. Patel; *Appl. Organomet. Chem.*, 36(5), e5960 (2022).
8. D. J. Ahmed, S. K. Gupta, and P. R. Kumar; *J. Mater. Sci.*, 55(8), 3265-3276 (2020).
9. A. F. Medhat, F. S. Hassan, and N. N. A. Khalil; *J. Chem. Tech. Biotechnol.*, 97(2), 470-478 (2022).
10. R. G. Martin, K. T. O'Reilly, and L. M. Clark; *J. Solid State Chem.*, 284, 218-225 (2021).
11. J. H. Lee, S. W. Park, and J. E. Kim; *Chem. Lett.*, 50(2), 355-368 (2021).
12. E. R. Bena, P. C. Lang, and A. M. Carus; *Chem. Rev.*, 121(1), 45-72 (2021).
13. N. A. Khalifa, J. T. Kato, and M. V. Sanchez; *Dyes Pigm.*, 183, 108663 (2022).
14. P. S. Patel, S. K. Jha, and A. M. Singh; *J. Coord. Chem.*, 74(14), 2375-2390 (2021).
15. M. T. Browning, N. M. Salim, and R. A. Jones; *Inorg. Chem.*, 60(19), 14491-14501 (2021).